Monte Carlo Simulations of the Mechanism for Channel Selectivity: The Competition between Volume Exclusion and Charge Neutrality

Dezsö Boda

Department of Physical Chemistry, University of Veszprém, H-8201 Veszprém, P.O. Box 158, Hungary

David D. Busath

Department of Zoology and Center of Neuroscience, Brigham Young University, Provo Utah 84602

Douglas Henderson*

Department of Chemistry and Biochemistry, Brigham Young University, Provo Utah 84602

Stefan Sokołowski

Department for the Modeling of Physico-Chemical Properties, MCS University, 20031 Lublin, Poland

Received: May 31, 2000; In Final Form: July 25, 2000

A mechanism for selectivity of calcium over sodium in a biological channel is studied by means of a Monte Carlo simulation. This model channel is an infinite cylinder containing negatively charged glutamates, each modeled as a pair of half charged oxygens, and an electrolyte. The fluid in the channel is in equilibrium with a bulk electrolyte. The proportion of Ca^{2+} ions in the channel is greatly in excess of that in the bulk because, in the restricted space in the channel, the doubly charged Ca^{2+} ions require less volume and are more effective at neutralizing the charge of glutamates than twice the number of singly charged Na^{+} ions with the same amount of charge.

Introduction

Voltage-gated calcium channels are found in heart, smooth muscle, and nerve cell membranes are critical for cell activation and signaling.[1] For example, in heart and smooth muscle cells, they prolong the action potential to allow long synchronous contractions. At the nerve terminal, they transduce the action potential to cause release of neurotransmitter. In the sarcoplasmic reticulum, calcium release channels are activated to release calcium to activate actin/myosin contraction.

The three-dimensional atomic structure of calcium channels is not known. However, the amino acid sequence and structure in calcium channels is similar to that of voltage-gated sodium channels, with four repeats, each containing six transmembrane helices, and a pore-lining loop, called the P region.[2] The P regions from the four repeats combine into a sleeve, forming a shallow selectivity filter near the extracellular side of the protein. Because of topological similarity to the bacterial KcsA potassium channel, whose crystal structure is known,[3] it is probable that the selectivity filter opens into a nonselective cavity and then a passageway lined by α helices, through which the ions finally enter the cell.

Site-directed mutagenesis studies have proven that glutamates at the tips of each of the four P-region loops are responsible for calcium channel selectivity.[4] In the calcium channel selectivity filter, the four glutamate residues (if unprotonated) would bear a net charge of −4, whereas in the sodium channel, the homologous residues (Asp, Glu, Lys, and Ala) would have a net charge of −1. This strongly suggests that confinement of a large negative charge in a small volume is responsible for selective binding and permeation of divalent cations in calcium channels.

This concept is consistent with a large body of data on ion binding by proteins, such as calcium binding proteins, and chelators, such as ethylenediamine tetraacetic acid (EDTA). However, the ion channel presents a confined geometry of approximately cylindrical structure, for which somewhat different physical principles may come into play, so it is appropriate to evaluate the binding affinity of such a charged space, which we do here using a statistical mechanical simulation.

In earlier studies of the equilibrium between bulk solutions and model charged capillaries, it was assumed that the channel contents must neutralize exactly the charge within the capillary.[5] However, recent studies[6] have pointed out that violations of local charge neutrality in pores (but not in the full system) may occur. Molecular dynamics simulations using charge perturbations on the permeating ion were carried out previously for a set of glutamates projecting into a protein structure called a beta barrel, intended to simulate the calcium channel,[7] but the energies were incompatible with experiment, probably because of a lack of ions in the bath. Similar computations were performed recently by Ganesh et al.,[8] using a set of four acetates to simulate the glutamates, but similarly lacked ions in the bath.

Nonner et al.[9] (NCE) applied the excess chemical potential computed using a statistical mechanical theory, the mean spherical approximation (MSA), to the problem of the equilibrium density of a broad selection of ions, mainly Ca^{2+}, Na^{+} and Cl^{-}, in a cylindrical model of a calcium channel selectivity

* To whom correspondence should be addressed. E-mail: doug@huey.byu.edu.

10.1021/jp0019658 CCC: $19.00
Published on Web 08/25/2000

filter and came to the important conclusion that Ca^{2+} was preferentially selected because of the interplay of charge and volume exclusion; the number of sodiums, naturally attracted by the four glutamates (represented as eight-half charged oxygen anions), would take up more volume than available in the interior of the channel, whereas the same amount of charge can be delivered in half the volume by Ca^{2+}. We may refer to this as a charge/space competition (CSC) mechanism. The CSC mechanism can be considered to be a generalization of the Hille-Eisenman dehydration/field strength matching mechanism for sodium channel selectivity.[1] However, the NCE approach suffers from the direct application of MSA chemical potentials, appropriate for a large isotropic volume, to a confined anisotropic space, the channel interior.

Here, we report the results of MC simulations for the ion occupancy of a cylindrical volume containing mobile (but confined within the channel) half charged oxygen anions of an appropriate density at different bath Ca^{2+} concentrations. Each pair of half charged oxygen anions represents a carboxylate group in glutamate. The method we use is to surround an infinite cylinder with a large solution containing a sufficient number of ions to represent a bulk solution (the bath). Monte Carlo moves are carried out until the system has equilibrated and the interior is in equilibrium with the external solution. We then average over a chain of subsequent moves. In the simulations, the Na^+ density in the bath is constant, but the Ca^{2+} and Cl^- densities are varied and the densities of the ions in the channel are assayed. This method is feasible only for moderate to high concentrations of Ca^{2+} in the bath because, to obtain adequate statistics, a minimum of several Ca^{2+} ions must be present in the computational cell. A low fraction of Ca^{2+} ions would require a very large number of Na^+ and Cl^- ions, resulting in excessively long computations. Thus, our simulations cannot access as large a concentration range as that used in the NCE approach. However, the critical region, where selectivity is demonstrated, is accessible, and the results are qualitatively similar in that range to those obtained by NCE, indicating that their approximations still allow a qualitatively correct result and justifies the CSC mechanism.

We expect that the CSC mechanism will play a significant role in selectivity between anions and cations, critical, for instance, for the opposite physiological functions of the cation-selective glutamate receptor channel and anion-selective glycine receptor channel.[1]

After this work was completed, we have become aware of a recent study of potassium channels. Goulding et al.,[10] have investigated a potassium channel using an infinite cylinder of variable diameter. Their primary focus was on volume exclusion effects. The selectivity of Na^+ and K^+ was studied. Because these ions have equal charge, but differ in size, electrostatics plays a relatively minor role in their study. They used simulations and density functional theory (DFT). As the diameter of the cylinder is varied, the selectivity of their model channel favors either K^+ or Na^+, depending upon the number of layers of these ions that can fit into the cylinder.

Model; Simulations

The geometry of the system that we consider is displayed in Figure 1. Note that the dimensions are not to scale. Nor are the numbers of spheres in the regions representative of the numbers of ions actually in these regions. The simulation cell has a cylindrical symmetry and consists of three concentric cylinders with hard walls. The inner cylinder, of radius R_1, models the wall of the channnel, and the space inside this cylinder defines

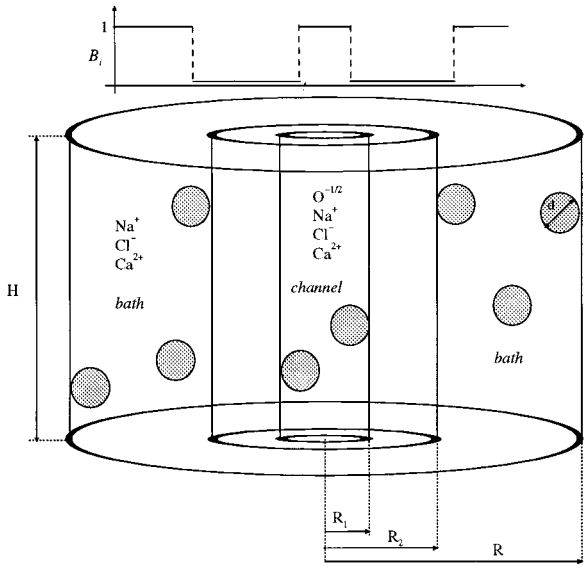

Figure 1. Geometry used in the simulations.

the aqueous pore. The next cylinder, of radius R_2, represents the barrier separating the channel and the bulk fluid, and the region between these two cylinders could be thought to be a simple minded model of the membrane or channel protein. The bulk fluid (or bath) is outside this wall and is in equilibrium with the fluid in the channel. In biological channels, the electrolyte in the regions outside the two channel entry points can be different. In our model, there is only one bath. Therefore, our model is applicable to experiments involving symmetrical solutions. The outer cylinder, of radius R, is applied to confine the whole simulation cell. This wall must be far enough from the outer membrane surface (i.e., $R - R_2$ must to be large enough) so that there is a flat, bulklike density profile in the middle of the region between R_2 and R. That is, $R - R_2$ must be large enough for this to occur but not so large as to make the simulation excessively time-consuming.

Periodic boundary conditions are applied in the z direction. Thus, the channel has an infinite length. Obviously, in reality the channel is not infinite in length. If the model channel had a finite length, both the radius and perpendicular (or axial) distance would be needed as variables. Although this would increase the computational time, this is not too great a complication in a simulation but would make the density functional theory (DFT) calculations, that we intend to make, more difficult. Because the whole point of DFT is its simplicity, this would be self-defeating. Furthermore, the model membrane should extend far beyond the channel. That is, $R_2 - R_1$ should be large. Our experience[11] with one-dimensional barriers in electrolytes suggests that the thickness of the region between the two cylinders need not be exceedingly large in order that the two regions are in equilibrium but otherwise nearly independent. Clearly, the geometry we use is an idealization.

The surfaces of the membrane can carry any constant surface charge. In this study, we assume that both walls are uncharged. That is, we assume that the charge on the wall of the channel protein is represented by the oxygen ions confined within the channel. In addition to the surface charge (zero in our case), a nonelectrostatic, short-range ion-wall van der Waals force acts upon the ions, described by

$$e^{-\beta v_i(r)} = \begin{cases} B_i, & R_1 - d/2 < r < R_2 + d/2 \\ 1, & \text{otherwise} \end{cases} \quad (1)$$

Thus, $v_i(r)$ is a square well potential for the ion of species i, d is the particle diameter (that, in this paper, is assumed to be

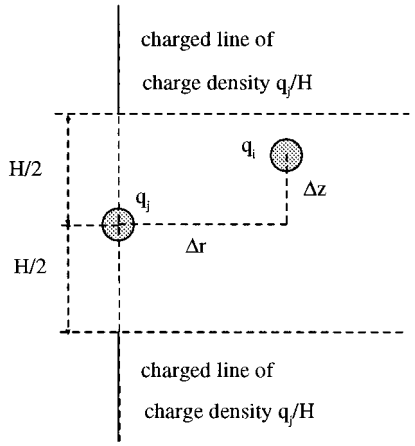

Figure 2. Illustration of the calculation of the potential between an ion with charge q_i and the charged lines belonging to an ion of charge q_j.

the same for all species), and B_i is the Boltzmann factor that determines the willingness of an ion to stay in the interior of the "membrane". In this study, the value of B_i is taken to be 0.001 for the ionic species (except for the oxygens); this means that the presence of the ions in the membrane is practically forbidden. The Boltzmann factor for the oxygens is identically zero everwhere, except within the channel, $r < R_1 - d/2$, where it is unity. The Boltzmann factor for the ions (other than the oxygens), as a function of r, is shown schematically on the top of Figure 1.

The ions are modeled as charged hard spheres; the interaction between the ions (including the oxygens) is

$$u_{ij}(r_{ij}) = \begin{cases} \infty, & r_{ij} < d \\ \dfrac{q_i q_j}{\epsilon r_{ij}} & r_{ij} > d, \end{cases} \tag{2}$$

where q_i is the charge of an ion of species i and r_{ij} is the separation of the ions. The solvent is represented by a dielectric continuum whose dielectric constant is $\epsilon = 78.5$. The value of the dielectric constant is everywhere identical. Because the protein molecules are polarizable, there is no reason the dielectric constant in the channel should be the same as in the bath. Nonner et al. chose a smaller value for the dielectric constant in the channel to obtain closer agreement with experiment. We have not done this as, in this study, we prefer to have as few arbitrary constants as possible.

The long-range contribution from the periodic images of the ions in the z direction is calculated on the basis of a one-dimensional version of the "sheet method" that was proposed by Torrie and Valleau.[12] This method has been developed further by Boda et al.[13] In the sheet method, the periodic images of an ion are replaced by a charged sheet, and the potential between an ion and this sheet can be integrated and expressed in a closed formula. Because the periodic boundary condition is applied in only one dimension, the periodic images of the central ion take place along a line, so we replace these images by a charged line. Consequently, we call this procedure the "line method".

Let us consider an ion of charge q_i and another one of charge q_j, shown in Figure 2. The periodic images of ion q_j are two strings of ions that are infinite in both the positive and negative z directions. These strings are replaced by uniformly charged lines (thick solid lines in Figure 2) carrying the charge density q_j/H, where H is the dimension of the simulation cell in the z direction. The long range correction to $u_{ij}(r_{ij})$ is obtained by calculating the interaction between the ion q_i and these charged lines. After integration, this term can be expressed as

$$u_{ij}^{LRC}(\Delta z,\Delta r) = -q_i \frac{q_j}{H}[\ln(H/2 + \Delta z + \sqrt{(H/2 + \Delta z)^2 + \Delta r^2}) + \ln(H/2 - \Delta z + \sqrt{(H/2 - \Delta z)^2 + \Delta r^2})] \tag{3}$$

In this equation

$$\Delta z = z_i - z_j \tag{4}$$

and

$$\Delta r = \sqrt{r_i^2 + r_j^2 - 2r_i r_j \cos(\theta_i - \theta_j)} \tag{5}$$

where r_i, θ_i, and z_i are the coordinates of ion i in the cylindrical coordinate system. Since the completion of this work, we have become aware of an earlier use of the line method.[14]

The electrolyte in the bath consists of Na^+, Ca^{2+}, and Cl^- ions. The electrolyte in the channel consists of these three species of ions plus the $O^{-1/2}$ ions. We assume that the ions are all equal in size with a diameter $d = 2.5$ Å. The solvent is represented by a dielectric continuum whose presence is manifest by a dielectric constant (the amount by which the field is decreased due to polarization) with a value everywhere of $\epsilon = 78.5$ (the value for water). We use $d = 2.5$ Å for the ionic diameters because it is a typical ion diameter and many of the experimental channel dimensions are (or nearly are) convenient integer multiples of this number. All distances are expressed as the distance divided by d. In subsequent studies, we will consider the effect of an electrolyte with ions with different ionic diameters and of a molecular solvent.

In the absence of calcium in the bath, it is known that calcium channels can pass large ions. For instance, tetramethylammonium is freely permeable,[15] implying that the narrowest diameter of the aqueous pore must be at least 6 Å. It is probable that the region that is relevant for selectivity has a larger diameter than 6 Å. Hence, we use a diameter $2R_1 = 10$ Å ($R_1 = 2d$) that is close to the diameter used by NCE. The radius of the outer wall is $R_2 = 15$ Å ($R_2 = 6d$). That is, the thickness of the region between the two cylinders is $4d$. The radius of the simulation cell was $R = 40d$. The length of the cell was $H = 20d$, $40d$, or $60d$, depending on the concentration of the Ca^{2+} ions in the bath and the concentration of oxygens in the channel.

As is conventional, we use reduced or dimensionless units for the temperature, T^* and reduced charge q^*. These are defined (in esu units) by

$$T^* = \frac{1}{q^{*2}} = \frac{\epsilon dkT}{e^2} \tag{6}$$

where e is the electronic charge. The definition in rationalized MKS units is similar, except that a factor of $4\pi\epsilon_0$ must be included in the definition. In our calculations, using $T = 300$ K for the temperature, $T^* = 0.352\,31$.

Monte Carlo simulations have been performed in a canonical ensemble, where the temperature, the volume, and the number of particles were fixed. A discussion of the Monte Carlo method may be found in any of the recent treatises[16] In the simulations, the concentration of the Na^+ ions in the bath was kept at a constant value of 0.1 M, which is typical for biological situations. We use dimensionless or reduced densities, obtained by multiplying the number density by d^3. For $d = 2.5$ Å, a 0.1

TABLE 1: Average Ionic Densities in the Channel

$\log_{10}[\rho^*_{bulk}(Ca^{2+})]$	$\rho^*_{channel}(Na^+)$	$\rho^*_{channel}(Ca^{2+})$	$\rho^*_{channel}(Cl^-)$	net channel charge
		no oxygens[$\rho^*_{channel}(O^{-1/2})=0$]		
$-\infty$	0.000 847	0.000 000	0.000 849	−0.000 002
−4.27	0.000 830	0.000 033	0.000 917	−0.000 020
−3.57	0.000 806	0.000 151	0.001 20	−0.000 091
		2 oxygens/d[$\rho^*_{channel}(O^{-1/2})=0.28$]		
$-\infty$	0.0787	0.0000	0.000 003	−0.0628
−6.75	0.0570	0.0117	0.000 005	−0.0612
−6.42	0.0488	0.0174	0.000 005	−0.0579
−5.51	0.0255	0.0332	0.000 014	−0.0496
−4.48	0.0092	0.0481	0.000 047	−0.0362
−4.09	0.0065	0.0514	0.000 070	−0.0322
−3.88	0.0052	0.0534	0.000 089	−0.0297
−3.74	0.0044	0.0547	0.000 120	−0.0278
−3.54	0.0037	0.0556	0.000 143	−0.0267
		4 oxygens/d[$\rho^*_{channel}(O^{-1/2})=0.56$]		
$-\infty$	0.1774	0.0000	0.000 000	−0.1055
−8.45	0.0824	0.0530	0.000 000	−0.0945
−7.05	0.0535	0.0706	0.000 000	−0.0882
−5.48	0.0106	0.1036	0.000 001	−0.0651

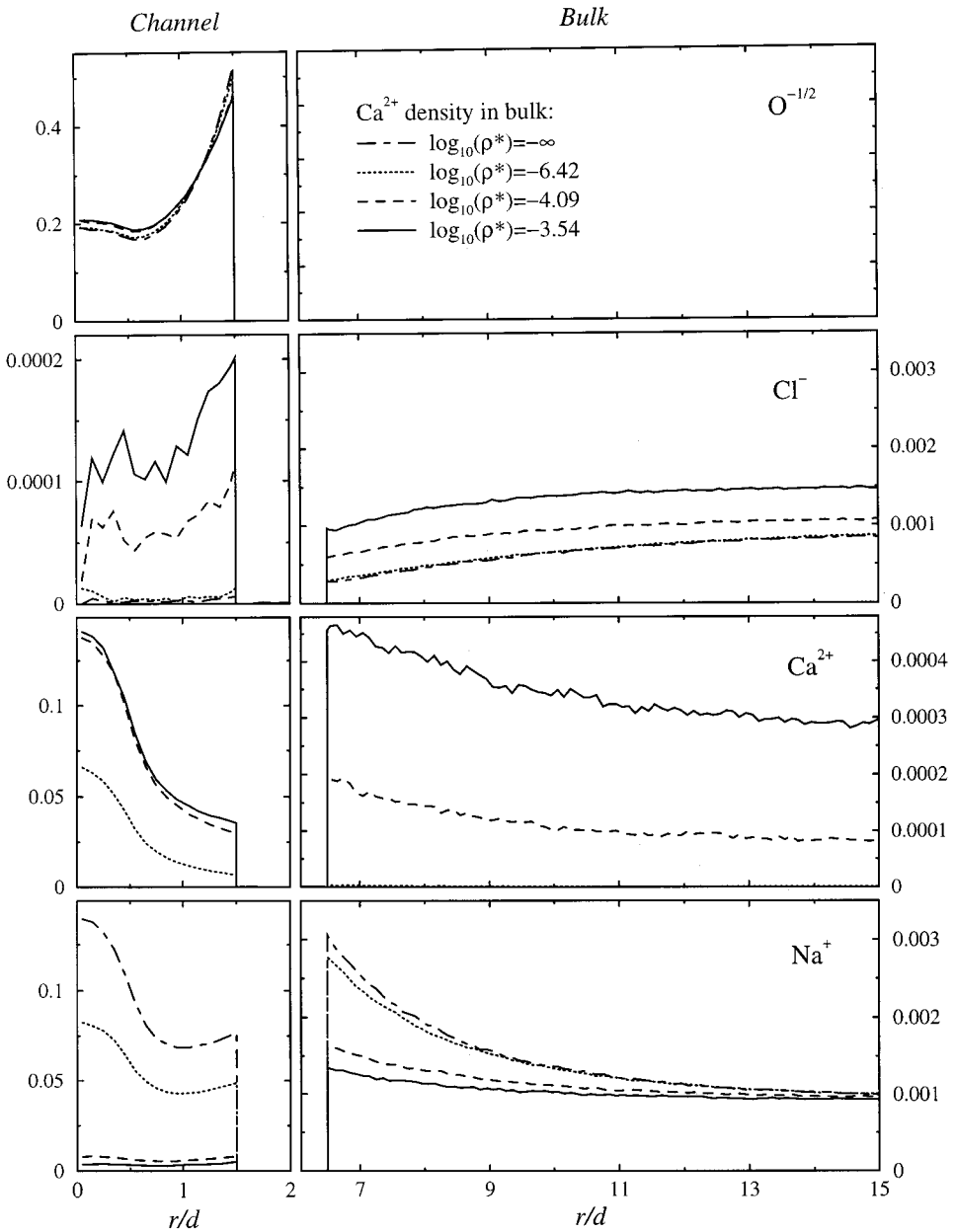

Figure 3. Ion densities as a function of radial distance, in units of d for the case of 2 $O^{-1/2}$ per distance d. The reduced or dimensionless ion densities are in units of d^3. Ion densities can be converted to mol/liter by dividing by 0.0094.

M NaCl has a reduced density $\rho^*(Na^+) = \rho(Na^+)d^3 = 0.000\ 94$. Thus, the density of each ion species in mol/liter is is obtained by dividing the reduced density by 0.0094. To ensure that this condition of constant Na^+ density is satisfied as closely as possible, the numbers of particles must be chosen appropriately. For this, a few test simulations were performed before the production runs to find the correct numbers of particles. The number of other ions was chosen so that, overall, charge neutrality was maintained. In this manner, the Na^+ bulk density was obtained with about $\pm$ 5% uncertainty. Hence, the densities of the other species in the channel and the bath have similar uncertainties. Despite these small uncertainties, the main conclusions concerning selectivity drawn from these simulations are unaffected.

A grand canonical ensemble (GCE) simulation would be preferable but particle insertions in the channel can be difficult at high density. In addition, separate simulations would be required to establish the chemical potential. The above mechanism is a reasonable compromise. We expect to make some DFT calculations for this model. Density functional theory is formulated in the GCE. On the basis of our earlier study[17] of a one-dimensional membrane, we expect that the mechanism that we have used for bringing the contents of the channel and bath into equilibrium will be confirmed by these DFT studies.

The procedure that we followed in our simulations is the following: A fixed number of half charged oxygen anions (representing the carboxylate groups of the channel protein) were placed into the channel. Then appropriate numbers of Na^+ and Cl^- ions were put into the cell to ensure charge neutrality in the system. The system was simulated for zero concentration of the Ca^{2+} ions. In the subsequent simulations, $CaCl_2$ was added to the system in increasing number. In each simulation, the number of Na^+ ions was chosen to ensure $\rho^*(Na^+) = 0.000\ 94$ in the middle region of the bath. The density profiles, as functions of r, and the average densities of the various species of ions in the channel and in the bath were calculated for each case.

It is important to note that in addition to the usual particle displacement, another Monte Carlo step was applied. Because the membrane is nearly impermeable to the ions, a long particle displacement, a "jump" between the channel and the bath, was used for the ions (other than the oxygens) to speed the equilibration between the channel and the bath.

Because this is an equilibrium calculation, we cannot calculate a current. However, we note that Nonner and Eisenberg[18] have suggested a method for computing currents when estimates of the electrochemical potential are made from equilibrium situations. We are unable to use this method here because we do not obtain electrochemical potentials. However, their method may be useful in our planned density functional theory study where the electrochemical potential is calculated.

We emphasize again that in reality channels have a finite length and the ions enter the channel through the ends. We shall study such a model in the future. However, the model studied here is a useful starting point that we believe captures the essence of the problem.

Results

We consider three cases. In one case, we assume that there are 8 $O^{-1/2}$ ions in the channel for a length for the selectivity filter of 5 Å (2d). This is the number used by NCE and gives a good model for the structure appropriate to the calcium channel structure, assuming no titration of glutamates (i.e., at pH 9), for the entire range of Na^+ and Ca^{2+} densities considered here.

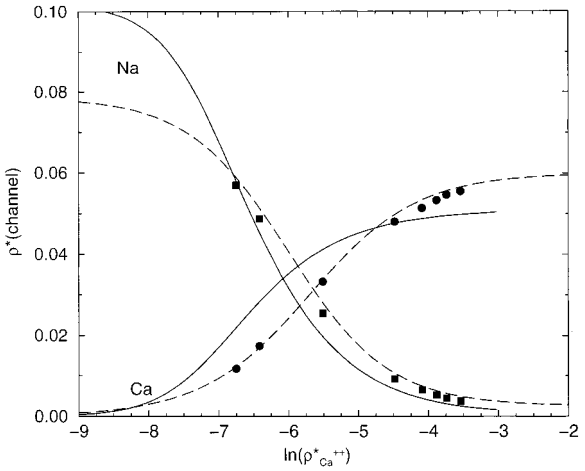

Figure 4. Average ion densities in the channel as a function of the bulk Ca^{2+} density for the case considered in Figure 3. The points give the simulation results, the solid curve gives the results of the NCE theory, and the broken curve gives the results of our fit. The squares and curves with a negative slope are for Na^+, whereas the circles and curves with a positive slope are for Ca^{2+}. The units are as in Figure 3.

It is interesting to consider a different concentration of oxygens (or carboxylates) for two reasons. First, the charge on the glutamates could be lower at neutral pH, assuming an upward shift in the titratability of glutamate. Additionally, the simulations are difficult for this large concentration of oxygens because the large negative charge tends to draw all the Ca^{2+} ions into the channel. To avoid this, we found it necessary to use a large simulation cell. Therefore, we also have examined the case where there are 6 $O^{-1/2}$ ions in the channel for a channel length of 7.5 Å (3d). This density is arrived at by assuming that the glutamates extend further along the axis of the channel and that one glutamate is protonated because of a locally reduced pH. Because this number turns out (unintentionally) to be exactly half that used by NCE, we add a third case in which there are no oxygens in the channel. This could be considered to be a rough approximation of the case of uncharged, or fully protonated, carboxylate groups at a pH $\ll$ 5.4. The densities, computed using the volume of the channel that is accessible to the centers of the ions, are 0.28 and 0.56 for the cases of 2 oxygens/d and 4 oxygens/d, respectively. That is, we average over a radius of 3.75 Å that excludes the region next to the channel wall, where the ion centers cannot penetrate.

The simulation results for the average densities of the ions in the channel and bulk for the three cases are given in Table 1. Density profiles and average channel densities are given in Figures 3 and 4 for the case where there are 2 oxygens/d. Similar results for 4 oxygens/d are displayed in Figures 5 and 6. It is seen that when $O^{-1/2}$ ions are present in the pore, the channel is selective for Ca^{2+} ions over Na^+ ions. Further, the more charged oxygen ions, the greater the selectivity. When there are no charged oxygen ions in the channel, the channel is not selective and the density of Ca^{2+} ions in the channel is roughly proportional to the density of Ca^{2+} ions in the bath. In agreement with NCE, the Ca^{2+} ions tend to bring a small number of Cl^- ions with them into the channel.

An examination of the density profiles in Figures 3 and 5 is interesting. Inside the channel, the oxygens, which have the highest density in the channel, are generally near the edge of the channel. This, presumably, results from their mutual repulsion. In contrast, the Ca^{2+} and Na^+ ions tend to reside near the center of the channel. The Cl^- ions also tend toward the outside of the channel. Hence, the ion "pairs" tend to be

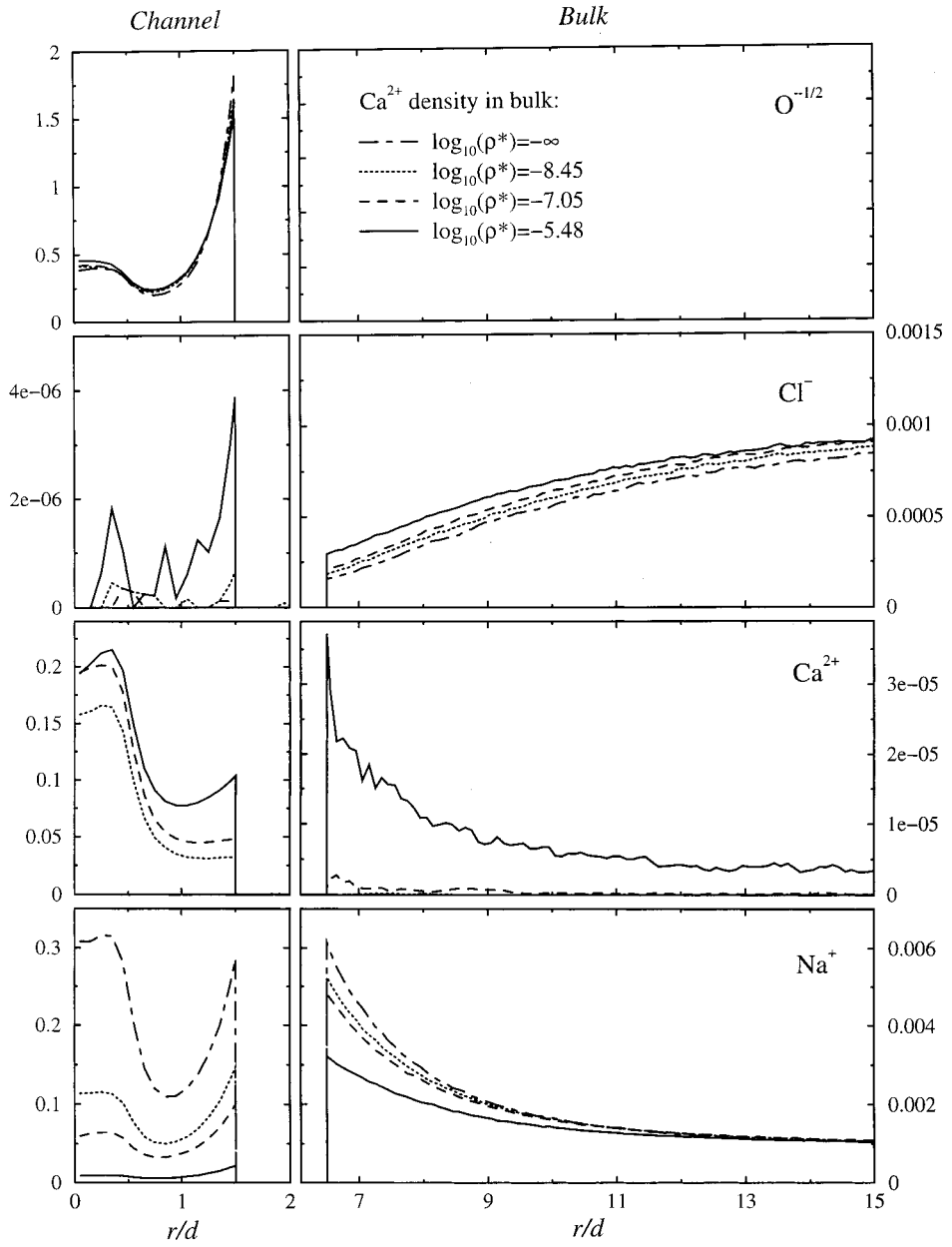

Figure 5. Ion densities as a function of radial distance for the case of 4 $O^{-1/2}$ per distance *d*. The units are as in Figure 3.

aligned radially. The ion profiles for the ions in the bath show some dependence on the presence of the negatively charged oxygens. The cations are attracted to the outside of the outer cylinder, whereas the anions are repelled. The density profiles of the ions in the bath can be quite noisy due to their low density and the small number of statistical samples.

From both Table 1 and Figures 3 and 5, we see that local charge neutrality is not satisfied completely within the channel; there is always a net negative charge in the interior of the channel. However, as Ca^{2+} ions are adsorbed into the channel, the degree to which local charge neutrality is satisfied increases. The net charge in the channel is greater for the higher density of O's.

We have fit the simulation results for the average ion densities $\rho(x)$, in the channel that are shown in Table 1 to the function

$$\rho(x) = \frac{\rho(-\infty) + c\rho(\infty)}{1 + c} \tag{7}$$

or, equivalently, to a form similar to a competition binding isotherm that is commonly used in biophysics

$$\rho(y) = \frac{\rho(0) + c\rho(\infty)}{1 + c} \tag{8}$$

where $x = \log_{10} y$, $y = \rho_{bulk}(Ca^{2+})$, and $c = \exp[\alpha(x - x_0)] = (y/y_0)^{\alpha \ln 10}$. The parameter, y_0, is the mid-saturation density for channel Ca^{2+} or the mid-inhibition density for channel Na^+, and α is a steepness factor, analogous to the Hill coefficient that reflects the "order" of the "reaction" for sites that allow multiple occupancy by a single ligand.

This expression is a modest generalization of the familiar binding isotherm because multiple ion "binding", involving a mixture of species, occurs. The values of the parameters is given in Table 2. Our fit was not made using a least-squares criterion (or any other systematic criterion). We merely adjusted the parameter values until the curves looked much like the simulation results.

The primary finding from Figures 4 and 6 is that as the concentration of Ca^{2+} is increased in the bath, Ca^{2+} replaces

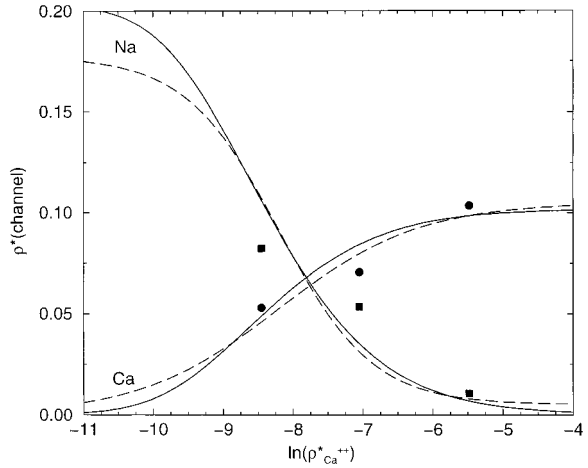

Figure 6. Average ion densities in the channel as a function of the bulk Ca^{2+} density for the case considered in Figure 5. The units are as in Figure 3. The meaning of the curves and points is as in Figure 4.

TABLE 2: Parameters Used in Eqs 7 and 8

species	$\rho^*(-\infty)$	$\rho^*(\infty)$	x_0	α
		2 oxygens/*d*		
Na^+	0.0787	0.0025	−6.0	1.4
Ca^{2+}	0.0000	0.0600	−5.7	1.3
		4 oxygens/*d*		
Na^+	0.1774	0.005	−8.2	1.5
Ca^{2+}	0.0000	0.105	−8.2	1.0

Na^+ in the channel at a lower concentration of Ca^{2+} when the density of oxygens is higher. The values of x_0 in Table 2 suggest that the midpoint occurs at reduced densities of Ca^{2+} in the bath of between 10^{-6} (10^{-4} M) for the low $O^{-1/2}$ density case and 10^{-9} (10^{-7} M) for the high $O^{-1/2}$ density case. These values bracket the high affinity Ca^{2+} dissociation constant, (10^{-6} M), postulated from kinetics models.[19] However, there is no indication of a distinct weak second ion 'binding' process with a dissociation constant of 10^{-2} M that is postulated to explain channel conductance levels and anomalous mole fraction effects. This suggests that some other process is involved that enhances the Ca^{2+} exit rate from the channel under physiological conditions.

Note that as we have stated above, the simulation results can be obtained only for larger values of the density of the added Ca^{2+} ions. This emphasizes the need for simpler theories, such as that of NCE and DFT, so that the adsorption of Ca^{2+} ions in the channel can be studied when the Ca^{2+} ion densities in the bath are very low.

It is of interest to compare the results of the NCE theory with our simulations. This comparison is a little ambiguous because the definition for the volume of the channel that is appropriate in their theory is uncertain. The definition of the density is quite clear in the simulations but is less clear in the NCE approach because it uses the properties of a bulk fluid rather than those of a confined fluid. Should their theory use the volume accessible to the centers of the spheres in the channel or is it the volume of the channel? For the purpose of comparison with our simulation results, Nonner used an average of these two possiblities. This uncertainty means that the comparison of the NCE theory with our simulations can only be qualitative. In any case, a comparison is made in Figures 4 and 6. The initial adsorption of the Na^+ ions may be higher in the NCE theory than in the simulations. However, given the fact that the simulations cannot access this region, this difference is insignificant. The saturation adsorption of the Ca^{2+} ions is lower in the NCE theory for the low oxygen density case (Figure 4) but similar in the high oxygen density case (Figure 6). Interestingly, the crossover points are given quite well. Given the fact that the NCE approach is not really a theory of an inhomogeneous fluid, the agreement of this theory with the simulations is quite good.

4 Summary

We have reported a simulation study of a model membrane channel that is selective for calcium ions. The selectivity results from an interplay between the volume exclusion effects due to the narrow channel diameter and the negative charge on the glutamates. We know that the size of the channel is important because, due to a programming error, we accidentally made some calculations for a 5*d* radius channel. This wider channel was Ca selective, but much less so than the 5 Å channel, whose results are reported here. The question of whether this reduction in the selectivity was due directly to the increased diameter in the channel or merely a reflection of the reduced density of the carboxylates is interesting. The diameter of the channel does not enter directly in the NCE theory. The selectivity in the NCE approach is mainly a function of the density of the carboxylates. However, volume exclusion does play a role in their theory because they find the selectivity of the channel for Ca^{2+} is greater than for the larger Ba^{2+} ions even though both ions have the same charge. The volume exclusion in the NCE theory comes only from the effect of volume exclusion on the bulk fluid chemical potentials. The fact that a large ion may have difficulty in entering a narrow channel does not arise in the NCE theory. We plan to investigate the diameter dependence of the selectivity of the model channel by varying the channel diameter while keeping the density of the carboxylates constant.

Because of the volume constraints in the narrow channel, Ca^{2+} ions are much more effective at neutralizing the negative charges on the glutamates. One Ca^{2+} ion is as effective as are two Na+ ions but needs only half the space. This is affected somewhat by the tendency of the Ca^{2+} ions to drag a few Cl^- ions with them. However, real Cl^- ions are rather large. In future calculations, where we use actual ion diameters, the Cl^- ions will be large and will have some difficulty in entering into the already crowded channel. As a result, we expect fewer Cl^- ions to enter the channel, and this may change the Ca^{2+} selectivity slightly. It is to be kept in mind that it is not necessary for charge neutrality to be exactly satisfied in the channel.[6] All that is required is that charge neutrality be satisfied in the entire system.

This study clearly confirms the predictions of the NCE approach, based on the use of the MSA for a homogeneous fluid, and supports the idea that space competition in the presence of electrostatic forces is responsible for calcium "binding" selectivity. Assuming that the channel occupancy is directly related to channel permeablity, the CSC mechanism explains the crucial functional feature of this voltage-gated channel.

It will be interesting to make further simulations using different ion radii and a model solvent. These will be reported in due course.

Acknowledgment. This work was supported in part by the National Science Foundation (Grant No. CHE98-13729), by the donors of the Petroleum Research Foundation, administered by the American Chemical Society (Grant No. ACS-PRF 31573-AC9), by a NATO High Technology Collaborative Research Grant (Grant No HTECH, CRG 972915), and by the National

Institutes of health (Grant No A*I*23007). S. S. acknowledges support from KBN (Grant No. 3T09A02714). The authors are grateful to Bob Eisenberg for drawing our attention to his work with Nonner and Catacuzzeno and to Wolfgang Nonner for providing the results of the NCE theory that are displayed in Figures 4 and 6. D.H. acknowledges the enthusiastic discussions with Eisenberg and Nonner in Moab Utah, which contributed to the final form of this paper. The authors are also grateful to Nonner for drawing our attention to some typographical errors in the presentation of the data in the first draft of our paper. Last, we thank Kwong-yu Chan for informing us of reference 14 and for his comments.

References and Notes

(1) Hille, B. *Ionic Channels of Excitable Membranes*; Sinauer Associates: Sunderland, MA, 1992.

(2) Catterall, W. A. *Science* **1988**, *242*, 50.

(3) Doyle, D. A.; Cabral, J. M.; Pfuetzner, R. A.; Kuo, A.; Gulbis, J. M.; Cohel, S. L.; Chait, B. T.; MacKinnon, R. *Science* **1998**, *280*, 69.

(4) Heineman, S. H.; Terlu, H.; Stühmer, W.; Imoto, K.; Numa, S. *Nature* **1992**, *356*, 441. Kim, M. S.; Morii, T.; Sun, L. X.; Imoto, K.; Mori, Y. *FEBS Lett.* **1993**, *318*, 145. Yang, J.; Ellinor, P. T.; Sather, W. A.; Zhang, J. F.; Tsien, R. W. *Nature* **1993**, *366*, 158.

(5) Vlachy, V.; McQuarrie, D. A. *J. Phys. Chem.* **1986**, *90*, 3248. Sørensen, T. S.; Sloth, P. *J. Chem. Soc., Faraday Trans*. **1992**, *88*, 571.

(6) Lozada-Cassou, M. In *Fundamentals of Inhomogeneous Fluids*; Henderson, D., Ed. **1992**, Dekker: New York, Chapter 8. Lo, W.-Y.; Chan, K.-Y.; Lee, M.; Mok, K.-L. *J. Electroanal. Chem*. **1998**, *450*, 265.

(7) Bogusz, S. B. Ph.D. Thesis **1995**, Brown University.

(8) Ganesh, P. S.; Chanda, B.; Gupta, S. K.; Mathew, M. K.; Chandrasekhar, J. *Proteins* **2000**, *38*, 384.

(9) Nonner, W.; Catacuzzeno, L.; Eisenberg, B. *Biophys. J*. **2000**, accepted for publication.

(10) Goulding, D.; Hansen, J.-P.; Melchionna, S. *Phys. Rev. Lett*. **2000**, accepted for publication.

(11) Henderson, D.; Bryk, P.; Sokołowski, S.; Wasan, D. T. *Phys. Rev. B* **2000**, *61*, 3896.

(12) Torrie, G. M.; Valleau, J. P. *J. Chem. Phys*. **1980**, *73*, 5807.

(13) Boda, D.; Chan, K.-Y.; Henderson, D. *J. Chem. Phys*. **1998**, *109*, 7362.

(14) Murthy, C. S.; Bacquet, R. J.; Rossky, P. J. *J. Phys. Chem.* **1985**, *89*, 701.

(15) McCleskey, E. W.; Almers, W. *Proc. Nat. Acad. Sci. US* **1985**, *82*, 7149.

(16) Allen, M. P.; Tildesley, D. J. *Computer Simulation of Liquids*; Oxford University Press: Oxford, UK, 1987. Frenkel, D.; Smit, B. *Understanding Molecular Simulation*; Academic Press: San Diego, CA, 1996. Sadus, R. J. *Molecular Simulation of Fluids*; Elsevier: Amsterdam, NL, 1999.

(17) Boda, D.; Henderson, D.; Rowley, R.; Sokołowski, S. *J. Chem. Phys*. **1999**, *111*, 9382.

(18) Nonner, W.; Eisenberg, B. *Biophys. J*. **1998**, *75*, 1287.

(19) Almers, W.; McCleskey, E. *J. Physiol.* **1984**, *353*, 453. Hess, P.; Tsien, R. *Nature* **1984**, *309*, 453. Lansman, J. F.; Tsien, R. *J. Gen. Physiol*. **1986**, *88*, 293. Miller, C. *J. Gen. Physiol*. **1999**, *113*, 783.